Chemical Engineering Journal 155 (2009) 184–190

Contents lists available at ScienceDirect

Chemical Engineering Journal

journal homepage: www.elsevier.com/locate/cej

Kinetics and thermodynamics of lead (II) adsorption on lateritic nickel ores of Indian origin

M. Mohapatra*, S. Khatun, S. Anand

Hydro-Electro Metallurgy Department, Institute of Minerals and Materials Technology, Bhubaneswar, Orissa 761013, India

ARTICLE INFO

Article history:
Received 7 February 2007
Received in revised form 11 June 2008
Accepted 16 July 2009

Keywords:
Nickel laterite
Pb(II) adsorption
Isotherms
Activation energy

ABSTRACT

The lead adsorption from aqueous solution was studied in batch experiments using two typical Indian origin nickel lateritic ores having high (46.29%) and low iron content (28.56%) coded as NH and NL respectively. The adsorption was found to be strongly dependent on pH of the medium showing increase in uptake of Pb(II) from 11.0 to 53% and 8.2 to 44% for NH and NL samples respectively with the increase in pH in the range of 2.0–5.23. The time data generated at different temperatures for both the samples fitted well to second-order kinetic model and Elovich equation. The later is indicative of a chemisorption process. The +ve ΔH° values (8.90 and 10.29 kJ mol^{-1} for NH and NL samples) support the endothermic nature of adsorption. The +ve ΔS° values (28.56 and 29.40 kJ mol^{-1} K^{-1} for NH and NL respectively) suggest that the adsorption occurs with internal structural changes. The activation energy was estimated to be 7.6 and 3.12 kJ mol^{-1} for NH and NL respectively. The thermodynamic activation parameters were also evaluated using Eyring equation. The loading capacities of NH and NL were estimated to be 44.4 and 28.45 mg g^{-1} respectively under the experimental conditions: adsorbent concentration 2 g l^{-1}, time 30 min, temperature 308 K and pH 5.23. Data fitted well to Langmuir and Freundlich isotherm models for NH while in case of NL only Langmuir isotherm showed good fit. Due to high loading capacities and favorable kinetics, these materials can be utilized for Pb(II) removal from aqueous solutions.

1. Introduction

Pb(II) is one of the toxic heavy metal ions notably present in soil environments through atmospheric dusts and solid wastes from a variety of active and inactive sources [1]. Its presence in the environment as a result of extensive and wide applications of mining, chemical, electroplating, petroleum refining, paper and pulp industries poses serious health hazards to living organisms. The permissible limit for Pb(II) in wastewater given by the Environmental Protection Agency is 0.05 mg l^{-1} [2] and that of the Bureau of Indian Standards (BIS) is 0.1 mg l^{-1} [3]. Therefore, it is needed to reduce the amount of this ion particularly in wastewater streams of hydrometallurgical and other industries. Filtration, adsorption, reverse osmosis, solvent extraction, electro-kinetic and membrane separation techniques are used for removal of heavy metals from aqueous solutions [4–18]. Among them adsorption has been shown to be an economically feasible alternative method for removing heavy metals from wastewater and water supplies [11–18]. Low cost adsorbents are generally preferred for the removal of impurities from aqueous solutions/contaminated water. Therefore, the search for novel materials with high efficiency to remove heavy metals from water and industrial effluents is of environmental and industrial interest. Waste products such as waste from bauxite refining (red mud), fly ash [19], blast furnace slag [20], manganese nodule leach residue [21] have been studied as adsorbents for the removal of Pb(II) ions. However, no work has been reported on the use of low and off grade ores for adsorption purposes. The objective of this study is to investigate and explore the feasibility of using nickel lateritic ores of Orissa, India for adsorption of Pb(II). The iron content in the Indian ore varies between 20 and 50% whereas the nickel content varies between 0.5 and 1.2%. These ores have not been commercially exploited for nickel extraction till now due to low nickel content. However, considerable efforts have been made at Institute of Minerals and Materials Technology to beneficiate these ores for upgrading nickel content and for developing acid/ammoniacal based processes [22–25] but still these ores are lying unutilized. With a view to find an alternative application of these ores for effluent and wastewater treatment, the present work on removal of Pb(II) from aqueous solution was taken up.

2. Experimental

2.1. Materials

Bulk samples of typical low and high iron containing nickel laterites samples were collected from Sukinda, Orissa, India. The

* Corresponding author. Tel.: +91 6742581635x272.
E-mail address: mamatamohapatra@yahoo.com (M. Mohapatra).

1385-8947/$ – see front matter © 2009 Elsevier B.V. All rights reserved.
doi:10.1016/j.cej.2009.07.035

Nomenclature

q_e	equilibrium concentration on adsorbent, mg g^{-1}
r^2	linear regression coefficient
t	time, min
T	temperature, K
q_t	the amount of Pb(II) adsorbed per unit mass of the adsorbent at time t, mg g^{-1}
k_1	adsorption rate constant for pseudo-first-order kinetic equation, t^{-1}
k_2	adsorption rate constant for pseudo-second-order kinetic equation, g mg^{-1} min
E_a	activation energy, kJ mol^{-1}
R	gas constant
k_0	Arrhenius factor
k_B	Boltzmann's constant
h	Planck's constant
ΔG°	free energy of reaction, kJ mol^{-1}
ΔH°	enthalpy of reaction, kJ mol^{-1}
ΔS°	entropy of reaction, J mol^{-1} K^{-1}
$\Delta G^\#$	free energy of activation, kJ mol^{-1}
$\Delta H^\#$	enthalpy of activation, kJ mol^{-1}
$\Delta S^\#$	entropy of activation, kJ mol^{-1} K^{-1}

samples were ground and sieved to obtain 100% <100 μm (−150 Mesh BSS, British Standard Sieves). $Pb(NO_3)_2{\cdot}4H_2O$, H_3PO_4, tin granules, mercurous chloride used in the present work were of MERCK, India, while NaOH, HCl, H_2SO_4 were of BDH grade and, BDAS indicator was of s-d-fine chemicals.

2.2. Characterization of adsorbents

A weighed amount of sample was subjected to tri-acid digestion for wet chemical analysis. Iron was analysed volumetrically [26]. The pH_{pzc} of prepared sample was determined following Balistrieri and Murray method [27]. The X-ray diffraction (XRD) measurements were done over a range of 20–70° using Phillips Powder Diffractometer Model PW1830 with Co Kα radiation at a scan speed of 1.2°/min. Surface area was measured with Quantasorb 1750 instrument.

2.3. Adsorption experiments

The Pb(II) adsorption experiments were carried out in an horizontal shaker having provisions for temperature and agitation control. After proper dilutions Pb(II) analysis was done by Atomic Absorption Spectrophotometer (PerkinElmer Model 2380). For each experiment 50 ml of Pb(II) solution of desired concentration and pH was taken in 100 ml stoppered conical flask and a weighed amount of adsorbent was added to it. The contents were stirred at 160 rpm (revolutions per minute) for desired period of time at constant temperature. The kinetic of adsorption was studied at various temperatures while keeping the adsorbent dose as 2 g l^{-1}. For fitting adsorption isotherm the data was generated at different initial concentrations of Pb(II) (50–500 mg l^{-1}) while keeping the adsorbent dose fixed (2 g l^{-1}). In order to test the reproducibility, some of the experiments were carried in duplicate and the reproducibility was found to be within ±2%.

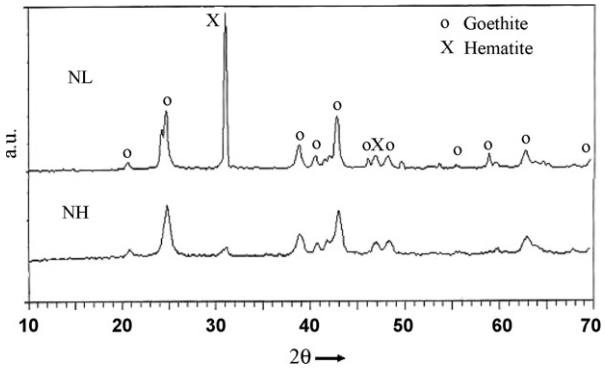

Fig. 1. XRD patterns of NH and NL samples.

3. Results and discussions

3.1. Chemical analysis and characterization

The physico-chemical analyses of two laterite samples are given in Table 1. For convenience the high iron containing sample has been coded as NH and the low iron containing one as NL. The XRD pattern (Fig. 1) shows goethite (α-FeOOH) (JCPDS, 1980, File No 29-713) as the major crystalline phase with 100% RI (relative intensity) peak at d value of 4.2 Å for NH sample. Some minor peaks corresponding to hematite (α-Fe_2O_3) (JCPDS, 1980, File No. 33-0664) are also observed. In case of NL sample, the XRD pattern shows both hematite and goethite as the major phases though the 100% RI peak at d value of 2.7 Å corresponds to hematite.

3.2. Effect of contact time at various pH

Effect of pH was studied in the range of 2–5.23 at 308 K with rest of conditions as: adsorbate concentration 100 mg l^{-1} and adsorbent concentration 2 g l^{-1}. The results at various pH are shown in Figs. 2 and 3 for NH and NL samples. The pH was not further increased as on keeping the 100 mg l^{-1} Pb(II) containing solution at a pH of 5.5, about 7% Pb(II) precipitated. With the increase in pH from 2 to 5.23, % Pb(II) adsorption increased from 11 to 53% for NH (Fig. 2) and from 8.2 to 44% for NL samples (Fig. 3). This could be due to increase in negative surface charge with increase in pH thereby facilitating cations adsorption. Furthermore, the proportion of hydrated ions increases with pH and these may have higher affinity as compared to the unhydrated Pb(II) ions [28]. Therefore, both these effects would contribute to higher cation adsorption with increase in pH. The results given in Figs. 2 and 3 show that equilibrium is attained in 60 min and no significant increase in adsorption is observed by further increasing the contact time. For rest of the experiments contact time was kept as 1 h.

Table 1
Physico-chemical properties of nickel laterites.

Sample	Chemical analysis, % metal*						Surface area (m^{2}g^{-1})	pH_{PZC}
	Fe	Ni	Cu	Co	Mn	Cr		
NH	46.29	1.15	0.04	0.07	1.06	2.24	74.67	6.95
NL	28.56	0.71	0.02	0.05	0.27	1.7	68.39	6.70

* All the metals are present as oxides/hydroxides. The iron is present as goethite and hematite. The balance will be acid insolubles which are 28.5% for NH and 55.3% for NL.

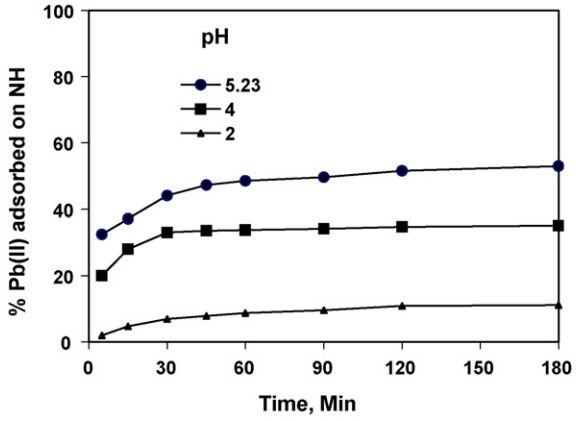

Fig. 2. Effect of contact time at various pH on adsorption of Pb(II) on NH: adsorbate concentration 100 mg l^{-1}, adsorbent concentration 2 g l^{-1}, temperature 308 K.

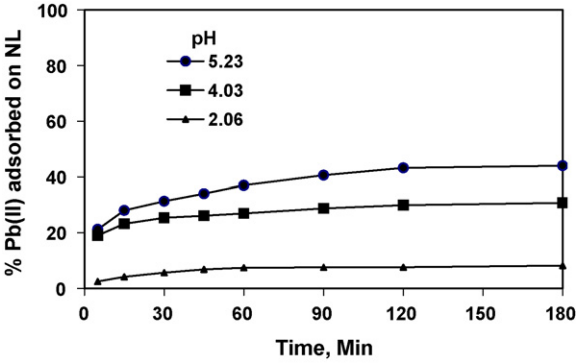

Fig. 3. Effect of contact time at various pH on adsorption of Pb(II) on NL: adsorbate concentration 100 mg l^{-1}, adsorbent concentration 2 g l^{-1}, temperature 308 K.

3.3. Effect of temperature

Effect of temperature was studied in the range of 308–338 K at a pH of 5.23 while rest of the conditions were kept as: Pb(II) 100 mg l^{-1} and adsorbent concentration 2 g l^{-1}. The adsorption data was generated for 60 min (Figs. 4 and 5). An increase in the temperature from 308 to 338 K led to an increase in % adsorption from 48.57 to 56% for NH and from 38.33 to 46.12% for NL samples. This is characteristic of a chemical reaction or bond being involved in the adsorption process. The increase in adsorption could be due to changes in pore size or an increase in kinetic energy of

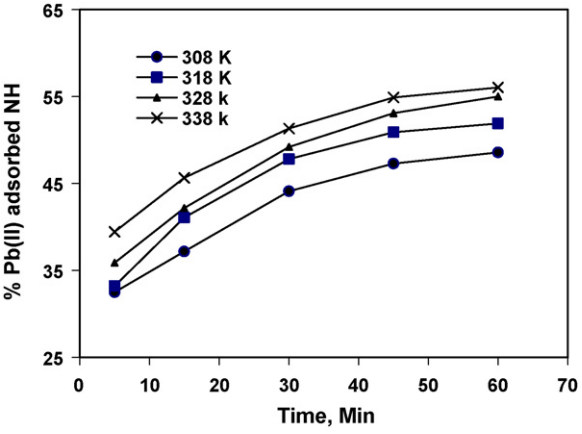

Fig. 4. Effect of temperature on adsorption of Pb(II) on NH: adsorbate concentration 100 mg l^{-1}, adsorbent concentration 2 g l^{-1} and pH 5.23.

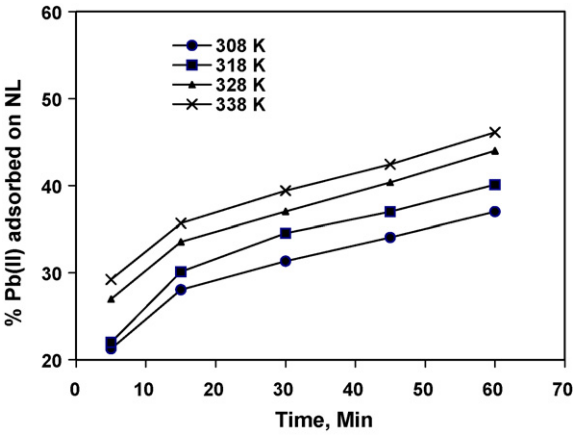

Fig. 5. Effect of temperature on adsorption of Pb(II) on NL: adsorbate concentration 100 mg l^{-1}, adsorbent concentration 2 g l^{-1} and pH 5.23.

the adsorbents. Such observations for adsorption of lead on iron oxide containing surfaces have been reported earlier [21,29,30]. The increase in % Pb(II) adsorption with increase in temperature suggests endothermic nature of adsorption which is attributable unequivocally to chemisorption [31].

3.4. Thermodynamic parameters

The thermodynamic quantities such as change in free energy (ΔG°), change in enthalpy of adsorption (ΔH°) and change in entropy (ΔS°) may give an insight about the nature and mechanism of adsorption process.

The values of ΔH° and ΔS° were determined from the Van't Hoff equation as given below.

$$\log K_c = \frac{\Delta S^\circ}{2.303R} - \frac{\Delta H^\circ}{2.303RT} \quad (1)$$

where R is the gas constant, T is the temperature (in Kelvin) and K_c is distribution coefficient and is determined as:

$$K_c = \frac{C_A}{C_e} \quad (2)$$

where C_e is the equilibrium concentration in solution (mg l^{-1}) and C_A is the adsorbed amount of adsorbate at equilibrium (mg l^{-1}) [32].

From the slopes and intercepts of the Van't Hoff plots (Fig. 6) ΔH° and ΔS° were calculated and are given in Table 2. Both ΔH° and ΔS° values are found to be positive suggesting a chemisorption process. During chemisorption, a certain amount of destructuring (i.e., desolvation) may be involved, creating a net positive entropy change and a slightly positive enthalpy of adsorption [33]. The positive value of adsorption entropy indicates the irreversible adsorption

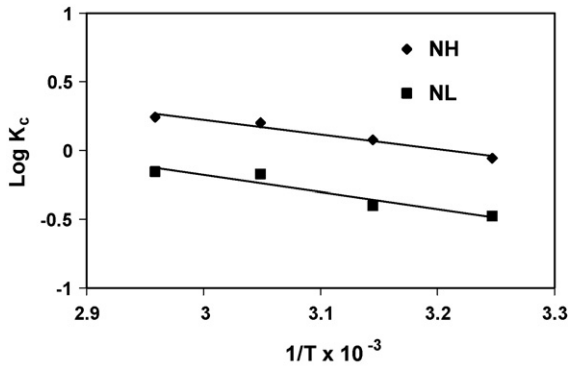

Fig. 6. Van't Hoff plots (data corresponds to Figs. 4 and 5).

Table 2
Thermodynamic and activation parameters of Pb(II) adsorption on NH and NL samples.

	NH				NL			
Temperature (K)	308	318	328	338	308	318	328	338
ΔG° (kJ mol^{-1})	0.103	−0.182	−0.467	−0.753	1.244	0.95	0.656	0.362
ΔH° (kJ mol^{-1} K^{-1})	8.90				10.29			
ΔS° (J mol^{-1})	28.56				29.40			
E_a	7.67				3.12			
$\Delta G^\#$ (kJ mol^{-1})	30.00	30.82	31.63	32.44	27.81	28.67	29.54	30.41
$\Delta H^\#$ (kJ mol^{-1} K^{-1})	4.99				1.1			
$\Delta S^\#$ (J mol^{-1})	−81.23				−86.71			

process, increased randomness at the solid–solution interface and stability of adsorption [33,34].

The free energy (ΔG°) values are calculated using the following equation:

$$\Delta G^\circ = \Delta H^\circ - T\Delta S^\circ \quad (3)$$

The free energy (ΔG°) values are given in Table 2. The ΔG° values are negative for NH except at 308 K. When the temperature increased from 318 to 338 K, the magnitude of free energy change (ΔG°) shifted to higher negative values. The ΔG° values for NL samples were +ve in the studied range of temperature.

3.5. Kinetics of adsorption

The experimental data of Figs. 4 and 5 were tested for best fits for pseudo-first-order Eq. (4) [35], the pseudo-second-order Eq. (5) [36] and Elovich Eq. (6) [37]. These equations are given below:

$$\text{1st order kinetics} \quad \ln(q_e - q_t) = \ln q_e - k_1 t \quad (4)$$

$$\text{2nd order kinetics} \quad \frac{t}{q_t} = \frac{1}{k_2 q_e^2} + \left(\frac{1}{q_e}\right) t \quad (5)$$

$$\text{Elovich equation} \quad q_t = \beta \ln(\alpha\beta) + \beta \ln t \quad (6)$$

From this simple form of Elovich equation, the parameters are estimated without using the origin ($q = 0$; $t = 0$).

Where q_e and q_t are the amounts of metal ion adsorbed per unit weight of adsorbent at equilibrium and at any time t, respectively (mg g^{-1}) and k_1 is the rate constant of pseudo-first-order sorption (min^{-1}). k_2 is the rate constant of pseudo-second-order adsorption (g mg^{-1} min). α is the initial adsorption rate of Elovich equation (mg g^{-1} min^{-1}), and the parameter β is related to the extent of surface coverage (mg g^{-1}) and activation energy for chemisorption [38]. The constants can be obtained from the slope and intercept of a straight line of q_t vs ln t.

The Pb(II) adsorption data given in Figs. 4 and 5 were treated to evaluate the rate constants at different temperatures for NH and NL samples. The data was first treated by first-order rate expression. The first-order rate constant, k_1, the regression coefficient r^2 and theoretical and experimental equilibrium adsorption capacity, q_e are given in Table 3. The $\log(q_e - q_t)$ vs time (t) plot (not shown) were linear with r^2 values varying from 0.972 to 0.987 for NH and from 0.944 to 0.993 for NL sample. However, the theoretical and experimental equilibrium adsorption capacities, q_e obtained from these plots varied widely. This indicates that this equation cannot provide an accurate fit of the experimental data. The data was then treated to pseudo-second-order kinetic plot (Eq. (5)). The t/q_t vs t plots are shown in Figs. 7 and 8 for NH and NL respectively. All the parameters obtained from these graphs are given in Table 3. The adsorption data for both the materials are found to fit well to pseudo-second-order kinetic as (i) the regression coefficients, r^2 for both NH and NL plots were ≥0.986, (ii) the theoretical as well as experimental q_e values matched very well ($\Delta q_e < 5\%$). An increase in temperature resulted in increase of q_e which is typical to chemisorption nature of adsorption [39,40]. Further the

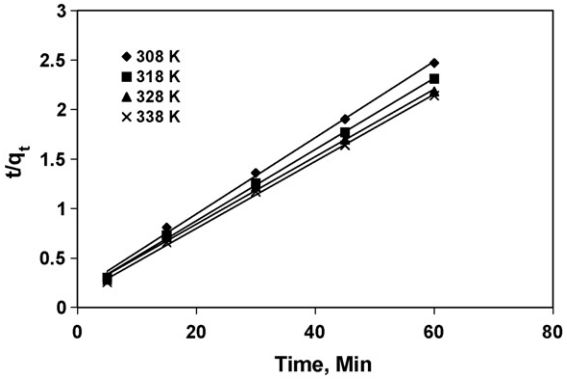

Fig. 7. Pseudo-second-order kinetic plots for NH (data corresponds to Fig. 4).

data was fitted to Elovich equation which is of general application to chemisorption kinetics. Many researchers [38–41] applied this kinetic model satisfactorily to the chemisorption processes. It is often valid for systems in which the adsorbing surface is heterogeneous. The Elovich plots (q_t vs ln t) are given in Figs. 9 and 10. The regression coefficients determined from these plots show good linearity for NH ($r^2 = 0.972$–0.993) and NL samples ($r^2 = 0.953$–0.986). The values of the coefficient α and β are also given in Table 3. With the increase in temperature, the constant α and β increased showing that both the rate of chemisorption and the available adsorption surface would increase. In conclusion, the pseudo-second-order model provides better correlation of the sorption data than the pseudo-first-order model, thus suggesting that the rate limiting step may be chemical sorption rather than diffusion.

3.6. Activation parameters

The values of the rate constant k_2 at different temperatures listed in Table 3 were applied to estimate the activation energy of the adsorption of Pb(II) onto NH and NL samples by the Arrhenius

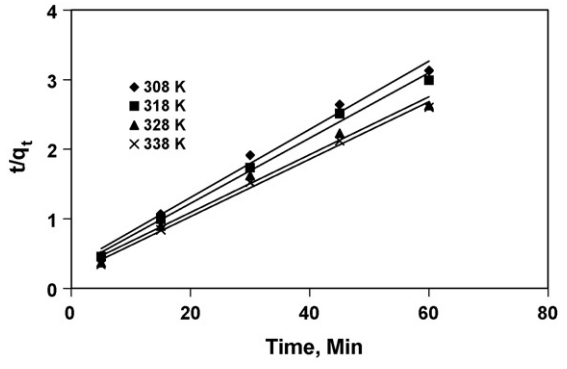

Fig. 8. Pseudo-second-order kinetic plots for NL (data corresponds to Fig. 5).

Table 3
Rate coefficients for adsorption of Pb(II) on NH and NL.

	NH				NL			
Temperature (K)	308	318	328	338	308	318	328	338
q_{exp} (mg g^{-1})	24.28	25.95	27.49	28.02	19.16	20.05	22.83	23.06
Pseudo-first-order								
$k_1 \times 10^{-2}$ (min^{-1})	6.4	7.2	5.75	6.48	3.33	3.59	3.04	3.68
q_e (mg g^{-1})	12.99	15.01	14.41	13.21	9.37	9.45	9.76	10.35
r^2	0.977	0.987	0.985	0.972	0.984	0.944	0.988	0.993
Pseudo-second-order								
$k_2 \times 10^{-3}$ (g mg^{-1} min)	3.14	3.39	3.73	4.09	7.3	7.75	7.95	8.25
q_e (mg g^{-1})	25.9	30.67	31.64	32.36	20.48	21.32	24.03	24.21
r^2	0.997	0.995	0.997	0.998	0.988	0.992	0.986	0.993
Elovich model								
α (g min^2 mg^{-1})	6.02	5.33	5.61	6.24	1.64	1.87	2.57	5.34
β (mg g^{-1} min^{-1})	10.31	11.93	12.31	13.13	5.31	5.53	7.55	9.19
r^2	0.972	0.993	0.985	0.991	0.973	0.983	0.953	0.986

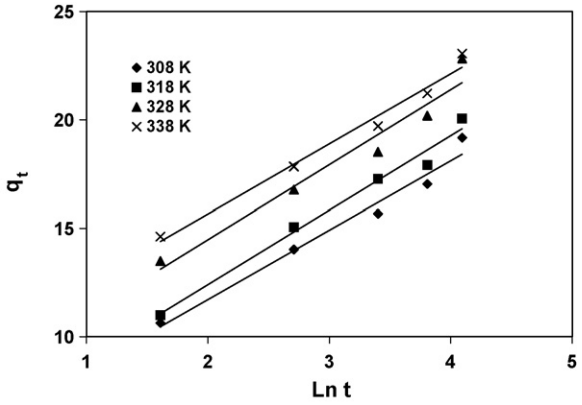

Fig. 9. Elovich kinetic plots for NH (data corresponds to Fig. 4).

equation [42] as follows:

$$\ln k_2 = -\frac{E_a}{RT} + \ln k_0 \quad (7)$$

where k_0 is the Arrhenius factor and R is the gas constant.

A straight line is obtained by plotting of the logarithm of the rate constant against the reciprocal of the absolute temperature (Fig. 11) and the activation energy E_a are listed in Table 2. The apparent activation energy of adsorption was found to be 7.6 and 3.12 kJ mol^{-1} for NH and NL, respectively (Table 2). These relatively low activation energy values obtained indicate that the adsorption of cations on the adsorbent surface is rapid; the rate limiting step being the migration of the cations to the adsorption site [43,44].

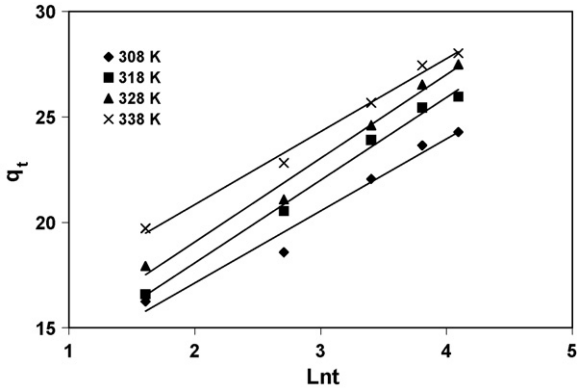

Fig. 10. Elovich kinetic plots for NL (data corresponds to Fig. 5).

To get an insight whether the adsorption process follows an activated complex, the enthalpy ($\Delta H^{\#}$), entropy ($\Delta S^{\#}$) of activation were calculated using Eyring equation (Eq. (8)) [45]. Free energy ($\Delta G^{\#}$) of activation was calculated using Eq. (9).

$$\frac{\ln k_2}{T} = \left(\frac{\ln k_B}{h_p} + \frac{\Delta S^{\#}}{R}\right) - \frac{\Delta H^{\#}}{RT} \quad (8)$$

$$\Delta S^{\#} = \frac{\Delta G^{\#} - \Delta H^{\#}}{T} \quad (9)$$

where k_B is Boltzmann's constant and h_p is Planck's constant, other parameters are defined earlier. From the slope and intercept of the graph $\ln k_2/T$ vs $1/T$ (Fig. 12), the enthalpy ($\Delta H^{\#}$) and entropy ($\Delta S^{\#}$) of activation were calculated. The enthalpy of activation, $\Delta H^{\#}$ values were 4.99 and 11.0 kJ mol^{-1} (Table 2) for NH and NL respectively. The magnitude and sign of $\Delta S^{\#}$ gives an indication whether the adsorption reaction is an associative or dissociative mechanism [46,47]. The negative value of $\Delta S^{\#}$ suggests that Pb(II) adsorption onto NH and NL is an associative mechanism.

3.7. Effect of Pb(II) concentration

With a view to generate adsorption isotherms, the initial concentration of Pb(II) was varied from 50 to 500 mg l^{-1} at a constant adsorbent concentration of 2 g l^{-1}, at pH of 5.23 and contact time of 60 min. The extent of adsorption decreased as expected from 69.77 to 17.77% for NH and from 46.72 to 11.38% for NL. The adsorption

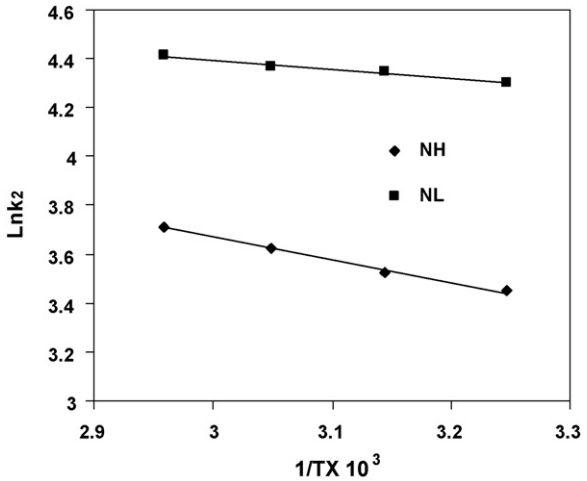

Fig. 11. Arrhenius plots: Pb(II) concentration 100 mg l^{-1}, adsorbent concentration 2 g l^{-1} and pH 5.23.

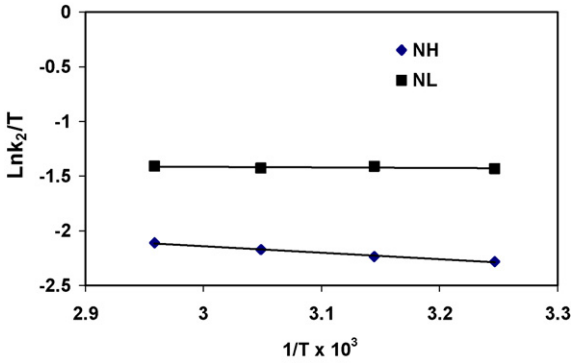

Fig. 12. Eyring plots: Pb(II) concentration 100 mg l^{-1}, adsorbent concentration 2 g l^{-1} and pH 5.23.

isotherms showing q_e vs Ce plots are given in Fig. 13. Under the experimental conditions the maximum loading capacities of NH and NL are found to be 44.4 and 28.45 mg g^{-1} respectively. Higher loading capacity of NH may be attributed to the high iron content of the sample.

3.8. Adsorption isotherms

Most widely tested isotherms for adsorption process are Langmuir and Freundlich models [48,49] which are given by Eqs. (10) and (11):

$$\text{Langmuir} \quad \frac{C_e}{q_e} = \frac{1}{bq_m} + \left(\frac{1}{q_m}\right) C_e \tag{10}$$

$$\text{Freundlich} \quad q_e = K_f C_e^n \tag{11}$$

where q_m, is the monolayer adsorption capacity (mg g^{-1}) and 'b', the constant related to the energy of adsorption (l g^{-1}), K_f indicates adsorption capacity (mg g^{-1}) and 'n' an empirical parameter related to the intensity of adsorption, which varies with the heterogeneity of the adsorbent. For "n"values in the range 1–10 ($0.1 < 1/n < 1$), adsorption is favorable. The greater the values of 'n' better is the favorability of adsorption.

According to Hall et al. [50], the essential features of the Langmuir isotherm can be expressed in terms of a dimensionless constant separation factor or equilibrium parameter R_L, expressed by Eq. (9).

$$\text{Separation factor } R_L = \frac{1}{1 + bC_e} \tag{12}$$

The isotherm is (i) unfavorable when $R_L > 1$, (ii) linear when $R_L = 1$, (iii) favorable when $R_L < 1$, and (iv) irreversible when $R_L = 0$. The value of R_L lie between 0 and 1 for favorable adsorption process

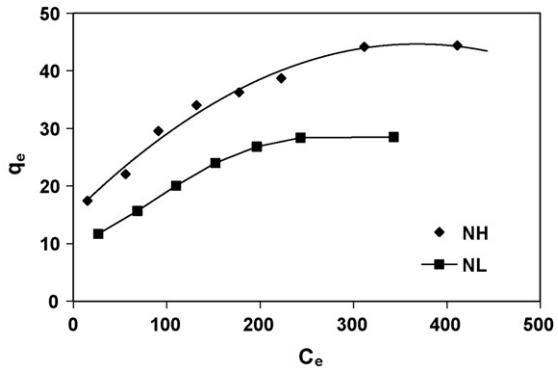

Fig. 13. Adsorption isotherms for NH and NL samples (q_e vs C_e): adsorbent concentration 2 g l^{-1}, pH 5.23 and temperature 308 K.

Table 4
Langmuir and Freundlich parameters for adsorption of Pb(II) on NH and NL.

Adsorbents	Langmuir coefficients				Freundlich coefficients		
	q_m (mg g^{-1})	b (l g^{-1})	r^2	R_L	K_f	n	r^2
NH	50.25	0.017	0.987	0.63	4.62	3.28	0.970
NL	33	0.017	0.991	0.53	5.18	2.84	0.940

[51]. The experimental data corresponding to Fig. 13 was treated for Langmuir and Freundlich models. The values of the adsorption coefficients obtained from the plots (not shown) are given in Table 4. The values of the Langmuir equilibrium coefficient, 'b', were found to be same (0.017 l g^{-1}) for both the samples. The Langmuir monolayer capacity, q_m, values were found to be 50.25 mg g^{-1} for NH and 33 mg g^{-1} for NL sample which are quite close to the experimental values. The separation factor R_L values of 0.63 and 0.53 for NH and NL respectively, indicate that the metal ions prefer to be in the bound state with surfaces [52]. The Freundlich isotherms (plot not shown) also yield good linear plots (r^2 were 0.97 and 0.94 for NH and NL). The Freundlich empirical coefficient, 'n' is found to be greater than one which indicates, adsorption intensity is high and adsorption occur through ion exchange process [53]. The fact that the adsorption of Pb(II) on NH and NL samples follow the Langmuir isotherm models indicates that a monolayer coverage is formed on the surface of the adsorbent [54]. Even though the Freundlich plot does yield a linear curve, the curve seems to bend at higher values of C_e, as the adsorption approaches a maximum value, confirming complete monolayer coverage of the adsorbent particles [34]. From these results the monolayer formation during adsorption of Pb(II) is confirmed.

3.9. Conclusions

Pb(II) adsorption on high and low iron containing laterite samples (NH and NL samples) increased with an increase in pH (2–5.23) and temperature (308–338 K). The adsorption kinetics followed pseudo-second-order model indicating towards chemisorption. Maximum Pb(II) adsorption at pH 5.23, temperature 308 K, initial Pb(II) concentration 400 mg l^{-1} were 44.4 and 28.4 mg Pb(II) g^{-1} of NH and NL samples respectively. The adsorption process was endothermic ($\Delta H = 8.90$ and 10.29 kJ mol^{-1} for NH and NL samples) accompanied by positive entropy ($\Delta S = 28.56$ and 29.40 kJ mol^{-1} deg^{-1}). The activation energy values (7.6 and 3.12 kJ mol^{-1} for NH and NL) indicate the adsorption occur via an activated chemisorption step with migration of cations to the adsorption site being the rate limiting step. The negative value of entropy of activation suggests that Pb(II) adsorption onto NH and NL is an associative mechanism. The adsorption data fitted well to both the Langmuir and Freundlich isotherms models. The isothermic data indicated monolayer coverage of Pb(II) on high and low iron containing laterites.

Acknowledgements

The authors are thankful to Director, Prof. B.K. Mishra, Institute of Minerals and Materials Technology (formerly Regional Research Laboratory), Bhubaneswar, for his kind permission to publish this paper. They wish to thank Dr. R.P. Das for useful discussions and Dr. R.K. Paramguru, Head, Hydrometallurgy Department. The financial support provided by Ministry of Environment and Forests (MOEF) is thankfully acknowledged.

References

[1] F.R. Siegel, Environmental Geochemistry of Potentially Toxic Metals, Springer-Verlag, Berlin, 2002.
[2] World Health Organization, Guidelines for drinking water quality, vol. 1 and 2, Geneva, Switzerland, 1984.
[3] Bureau of Indian Standards, Tolerance limits for industrial effluents prescribed by Bureau of Indian Standards, IS 2490 (Part I), New Delhi, India, 1981.
[4] G. Gode, E. Pehlivan, Removal of chromium(III) from aqueous solutions using Lewatit S 100: the effect of pH, time, metal concentration and temperature, J. Hazard. Mater. B136 (2006) 330–337.
[5] L. Zhang, J. Zhou, D. Zhou, Y. Tang, Adsorption of cadmium and strontium on cellulose/alginic acid ion-exchange membrane, J. Membr. Sci. 162 (1999) 103–109.
[6] H. Leinonen, J. Lehto, Ion exchange of nickel by iminodiacetic acid chelating resin Chelex 100, React. Funct. Polym. 43 (2000) 1–6.
[7] C.P. Huang, M.H. Wu, The removal of chromium(VI) from dilute aqueous solution by activated carbon, Water Res. 11 (1977) 673–679.
[8] D. Leppert, Heavy metal sorption with clinoptilolite zeolite: alternatives for treating contaminated soil and water, Min. Eng. 42 (1990) 604–608.
[9] S.K. Ouki, M. Kavannagh, Performance of natural zeolites for the treatment of mixed metal-contaminated effluents, Waste Manage. Res. 15 (1997) 383–394.
[10] G.C.C. Yang, S. Lin, Removal of lead from a silt loam soil by electro kinetic remediation, J. Hazard. Mater. 58 (1998) 285–299.
[11] S.B. Lalwani, T. Wiltowski, A. Hubner, A. Weston, N. Mandich, Removal of hexavalent chromium and metal cations by a selective and novel carbon adsorbent, Carbon 36 (1998) 1219–1226.
[12] R.S. Juang, R.C. Shiau, Metal removal from aqueous solutions using chitosan-enhanced membrane filtration, J. Membr. Sci. 165 (2000) 159–167.
[13] G. Yan, T. Viraraghavan, Heavy metal removal in a biosorption column by immobilized *M. rouxii* biomass, Bioresour. Technol. 78 (2001) 243–249.
[14] V.K. Gupta, C.K. Jain, I. Ali, M. Sharma, V.K. Saini, Removal of cadmium and nickel from wastewater using bagasse fly ash—a sugar industry waste, Water Res. 37 (2003) 4038–4044.
[15] V.K. Gupta, I. Ali, Removal of lead and chromium from wastewater using bagasse fly ash—a sugar industry waste, J. Colloid Interface Sci. 271 (2004) 321–328.
[16] D.P. Rodda, B.B. Johnson, J.D. Wells, The effect of temperature and pH on the adsorption of Copper(II), Lead(II), and Zinc(II) onto goethite, J. Colloid Interface Sci. 161 (1993) 57–62.
[17] C.E. Martinez, M.B. McBride, Dissolved and labile concentrations of Cd, Cu, Pb, and Zn in aged ferrihydrite-organic matter systems, Environ. Sci. Technol. 33 (1999) 745–750.
[18] A.R. Wilson, L.W. Lion, Y.M. Nelson, M.L. Shuler, W.C. Ghiorse, The effects of pH and surface composition on Pb adsorption to natural fresh water biofilms, Environ. Sci. Technol. 35 (2001) 3182–3189.
[19] R. Apac, E. Tutem, M. Hugul, J. Hizal, Heavy metal cation retention by sorbents (red muds and fly ashes), Water Res. 32 (1998) 430–440.
[20] S.V. Dimitrova, Metal sorption on blast-furnace slag, Water Res. 30 (1996) 228–232.
[21] A. Agrawal, K.K. Sahu, Systematic studies on adsorption of lead on sea nodule residues, J. Colloid Interface Sci. 281 (2005) 291–298.
[22] S.C. Panda, D.N. Dey, P.K. Rao, P.K. Jena, Extraction of nickel and cobalt from lateritic nickel ores of Orissa by pressure leaching with sulphuric acid, Trans. IIM 28 (1975) 483–487.
[23] G.V. Rao, T. Gouricharan, Process for enriching nickel from nickel containing overburden of chromite mines, Indian Pat. filed, NF/48/90 (1990).
[24] S. Anand, M.K. Ghosh, R.P. Das, Ammonia leaching of reduced nickel laterites, Internal report Aug 1991, RRL(B), Orissa, India, 1991.
[25] G.K. Das, S. Anand, S. Acharya, R.P. Das, Characterisation and acid pressure leaching of various nickel-bearing chromite overburden samples, Hydrometallurgy 44 (1997) 97–111.
[26] A.I. Vogel, A Text Book of Quantitative Inorganic Analysis, English Language Book Society and Longmans Green Publishers, Wiley and Sons, New York, 2000.
[27] L.S. Balistrieri, J.W. Murray, The surface chemistry of goethite (alpha-FeOOH) in major ion seawater, J. Am. Sci. 281 (1981) 788–806.
[28] G.W. Bruemmer, J. Gerth, K.G. Tiller, Reaction kinetics of the adsorption and desorption of nickel, zinc and cadmium by goethite. I. Adsorption and diffusion of metals, Eur. J. Soil Sci. 39 (1988) 37–52.
[29] W. Zou, R. Han, Z. Chen, Z. Jinghua, J. Shi, Kinetic study of adsorption of Cu(II) and Pb(II) from aqueous solutions using manganese oxide coated zeolite in batch mode, Colloids Surf. A: Phys. Eng. Aspects 279 (2006) 238–246.
[30] T. Kusuyama, K. Tanimura, K. Sato, Adsorption of heavy metal ions onto the surface of metal-incorporated hydrous ferric oxide particles, Mater. Sci. Forum 439 (2003) 210–214.
[31] W. Durnie, R. De Marco, A. Jefferson, B. Kinsella, Development of a structure-activity relationship for oil field corrosion inhibitors, J. Electrochem. Soc. 146 (1999) 1751–1756.
[32] M. Mohapatra, S. Anand, Studies on sorption of Cd (II) on Tata chromite mine overburden, J. Hazard. Mater. 148 (3) (2007) 553–559.
[33] D.J. Shaw, Introduction to Colloid and Surface Chemistry, Butterworth & Company, London, 1983, p. 109.
[34] D.B. Singh, G. Prasad, D.C. Rupainwar, Adsorption technique for the treatment of As(V)-rich effluents, Colloids Surf. A: Physicochem. Eng. Aspects 111 (1996) 49–56.
[35] S. Lagergren, Zur theorie der sogenannten adsorption geloster stoffe, Kungliga SVenska Vetenskapsakademiens, Handlingar 24 (1898) 1–39.
[36] Y.S. Ho, J.C.Y. Ng, G. McKay, Removal of lead(II) from effluents by sorption on peat using second-order kinetics, Sep. Sci. Technol. 36 (2001) 2711–2730.
[37] Y.S. Ho, G. McKay, Application of kinetic models to the sorption of copper(II) on to Peat, Adsorpt. Sci. Technol. 20 (2002) 797–815.
[38] H. Teng, C. Hsieh, Activation energy for oxygen chemisorption on carbon at low temperatures, Ind. Eng. Chem. Res. 38 (1999) 292–297.
[39] Y.S. Ho, G. McKay, The kinetic of adsorption of divalent metal ions onto sphagnum moss peat, Water Res. 34 (2000) 735–742.
[40] C.W. Cheung, J.F. Porter, G. Mckay, Adsorption kinetic analysis for the removal of cadmium ions from effluents using bone char, Water Res. 35 (2001) 605–612.
[41] M.X. Loukidou, A.I. Zouboulis, T.D. Karapantsios, K.A. Matis, Equilibrium and kinetic modelling of chromium (VI) biosorption by Aeromonas caviae, Colloids Surf. A 242 (2004) 93–104.
[42] J.W. Moore, R.G. Pearson, Kinetics and Mechanism, 3rd ed., John Wiley, New York, 1981.
[43] C.A. Eligwe, N.B. Okolue, C.O. Nwambu, C.I.A. Nwoko, Adsorption thermodynamics and kinetics of mercury (II), cadmium (II) and lead (II) on lignite, Chem. Eng. Technol. 22 (1999) 45–49.
[44] T. Robinson, B. Chandran, G.S. Naidu, P. Nigam, Studies on the removal of dyes from a synthetic textile effluent using barley husk in static-batch mode and in a continuous flow, packed-bed reactor, Bioresour. Technol. 85 (2002) 43–49.
[45] M. Al-Ghouti, M.A.M. Khraisheh, M.N.M. Ahmad, S. Allen, Thermodynamic behaviour and the effect of temperature on the removal of dyes from aqueous solution using modified diatomite: a kinetic study, J. Colloid Interface Sci. 287 (2005) 6–13.
[46] M. Dogan, M. Alkan, Adsorption kinetics of methyl violet onto perlite, Chemosphere 50 (2003) 517–528.
[47] K.G. Scheckel, D.C. Sparks, Temperature effect on nickel sorption kinetics of the mineral–water interface, Soil Sci. Soc. Am. J. 65 (2001) 719–728.
[48] I. Langmuir, The adsorption of gases on plane surfaces of glass, mica and platinum, J. Am. Chem. Soc. 40 (1918) 1361–1403.
[49] H.M.F. Freundlich, Over the adsorption in solution, J. Phys. Chem. 57 (1906) 385–470.
[50] K.R. Hall, L.C. Eagleton, A. Acrivos, T. Vermeulen, Pore- and solid-diffuion kinetics in fixed-bed adsorption under constant-pattern conditions, Ind. Eng. Chem. Fundam. 5 (1966) 212–223.
[51] S. Arivoli, B.R. Venkatraman, T. Rajachandrasekar, M. Hema, Adsorption of ferrous ion from aqueous solution by low cost activated carbon obtained from natural plant material, Res. J. Chem. Environ. 17 (2007) 70–78.
[52] T. Anirudhan, M. Sreedhar, Adsorption thermodynamics of Co(II) on polysulphide treated sawdust, Indian J. Chem. Technol. 5 (1998) 41–47.
[53] T.K. Sen, S.P. Mahajan, K.C. Khilar, Adsorption of Cu^{2+} and Ni^{2+} on iron oxide and kaolin and its importance on Ni^{2+} transport in porous media, Colloids Surf. A: Physicochem. Eng. Aspects 211 (2002) 91–102.
[54] M.F. Sawalha, J.R.P. Videa, J.R. Gonzalez, J.L.G. Torresdey, Biosorption of Cd(II), Cr(III) and Cr(VI) by saltbush (*Atriplex canescens*) biomass: thermodynamic and isotherm studies, J. Colloid Interface Sci. 300 (2006) 100–104.